LA-UR 91-556

LA-UR--91-556

DE91 008589

TITLE ON THE MEASUREMENT OF WIND SPEEDS IN TORNADOES WITH A PORTABLE CW/FM-CW DOPPLER RADAR

AUTHOR(S) Howard B. Bluestein and Wesley P. Unruh

SUBMITTED TO Tornado Symposium III

Los Alamos

Los Alamos National Laboratory
Los Alamos, New Mexico 87545

ON THE MEASUREMENT OF WIND SPEEDS IN TORNADOES WITH A PORTABLE CW/FM-CW DOPPLER RADAR

Howard B. Bluestein
School of Meteorology
University of Oklahoma
Norman, Oklahoma 73019

and

Wesley P. Unruh
Mechanical and Electronic
Engineering Division
Los Alamos National Laboratory
Los Alamos, New Mexico 87545

1. INTRODUCTION

Both the formation mechanism and structure of tornadoes are not yet well understood. The Doppler radar is probably the best remote-sensing instrument at present for determining the wind field in tornadoes. Although much has been learned about the non-supercell tornado from relatively close range using Doppler radars at fixed sites (Brady and Szoke 1989; Roberts and Wilson 1989; Wakimoto and Wilson 1989; Wilson and Roberts 1990), close-range measurements in supercell tornadoes are relatively few (Zrnic and Doviak 1975; Zrnic et al. 1977; Zrnic and Istok 1980; Zrnic et al. 1985).

Bluestein and Unruh (1989) have shown how a portable Doppler radar can increase significantly the number of high-resolution, sub-cloud base measurements of both the tornado vortex and its parent vortex in supercells, with simultaneous visual documentation. The design details and operation of the CW/FM-CW Doppler radar (Strauch 1976) developed at the Los Alamos National Laboratory (LANL) and used by storm-intercept teams at the Univ. of Oklahoma (OU) are described in Unruh et al. (1989), Bluestein and Unruh (1989), and Bluestein and Unruh (1990). The radar transmits 1 W at 3 cm, and can be switched back and forth between CW and FM-CW modes. In the FM-CW mode the sweep repetition frequency is 15.575 kHz and the sweep width 1.9 MHz; the corresponding maximum unambiguous range and velocity, and range resolution are 5 km, +/- 115 m s^{-1}, and 78 m respectively. The bistatic antennas, which have half-power beamwidths of 5°, are easily pointed with the aid of a boresight. CW data are recorded on stereo audio tape, while video is recorded on a boresighted VCR. FM-CW data are recorded on the VCR, while voice documentation is recorded on the audio tape; video is recorded on another VCR. The radar and antennas are easily mounted on a tripod, and can be set up by three people in a minute or two.

The purpose of this paper is to describe the signal processing techniques used to determine the Doppler spectrum in the FM-CW mode and a method of its interpretation in real time, and to present data gathered in a tornadic storm in 1990.

2. FM-CW SIGNAL PROCESSING

The time series of data are recorded in analog form on videotape, with each line representing both one sweep of the VCR and one full sweep in frequency of the radar. In real time the data are monitored on a video screen, as alternating light and dark bands. The range of the targets is inversely proportional to the spacing between the bands, and the target speeds are proportional to the slope of the bands; the direction of motion is given by the sign of the slope. More complex wind fields appear as cross-hatched lines. Range folding is manifest as an abrupt change in the slope of the lines. It is important when operating the radar to make sure that the picture on the screen is not torn up: this indicates that the signal is overloaded and the data unusable. Too weak a signal is indicated by a lack of any well-defined lines on the screen. The gain of the radar is easily set by a potentiometer.

Each of 128 consecutive lines from a video frame (there are 512 interlaced lines per frame, in addition to some "bookeeping" lines) are digitized into 128 data points. Although a high-pass filter is applied by the radar to attenuate ground clutter (wind speeds less than 3 m s^{-1} are significantly filtered out), the resulting time series of16384 data points is then filtered further by computing the *average* time series for the series of lines, and subtracting it from each line to obtain a perturbation time series.

The perturbation time series is range normalized, multiplied by a Hanning filter, and subjected to a discrete fast Fourier transform. The spectrum of the radial-wind component within each of 64 78-m range bins appears as a series of 128 data points, with the first of each, 64th, and 128th representing -115 m s^{-1}, 0 m s^{-1}, and +115 m s^{-1}, and so on. Data are not available from the first 39 m and from the last 39 m.

We verified that the radar was working properly in FM-CW mode by computing the spectra of our chase van moving at a constant speed away from and toward the radar, and noting the distance travelled by the van.

3. RESULTS: THE SPEARMAN, TEXAS STORM OF 31 MAY 1990

The largest of the tornadoes was in its mature stage when we were setting up the radar (Fig. 1). The entire cloud above, which extended up to the base of the storm's anvil, was rotating cyclonically and moving toward us from west to east; the area to the right (north) was relatively translucent, like in the typical low-precipitation (LP) supercell that occurs along the dryline (Bluestein and Woodall, 1990).

The CW spectrum of the tornado several min after the time of Fig. 1 is shown in Fig. 2; the spectrum is valid for an area centered on the tornado. We estimated the width of the tornado photogrammetrically to be about 200-300 m in diameter; the radar cross section was estimated to be slightly under 500 m. The spectrum shown is the average of 4 spectra taken over a 0.5 - 1 s period. The highest wind speeds measured, which are indicated where the spectrum enters the noise level, are about +/- 90 m s^{-1}. These wind speeds are consistent with the independent estimate of the NWS (National Weather Service) of F3 damage. Spectra of the area centered to the left and right of the tornado are shown in Figs. 3 and 4. The spectra are skewed toward the approaching side to the left, and toward the receding side to the right, as one would expect. The spectra shown in Figs. 3 and 4 suggest a parent vortex having wind speeds of approximately 30 - 40 m s^{-1} and a tornado having wind speeds as high as 80 - 90 m s^{-1}.

Figs. 5a and b show the FM-CW spectra for the remains of the rotating wall cloud from which the tornado was pendant earlier at longer range. The radar was pointed upward with an elevation angle of nearly 45°. Radar return from the wall cloud is evident from approximately 2.3 km to 3 km range; thus the width of the wall cloud was approximately 700 m. Wind speeds indicated were all about -35 m s^{-1}. This is consistent with the big blast from the southwest we felt as the wall cloud passed over us and 6-cm hail fell on us.

The integrated FM-CW spectrum for the wall cloud described above is shown in Fig. 6. It is to be compared with the CW spectrum shown in Fig. 7. Differences in the two may be attributed in part to slightly different times and viewing angles, and to possible problems with the data or data processing procedure. The peaks of the two spectra differ by approximately 5 m s^{-1}.

4. FUTURE WORK

In order to improve upon the effective range of the radar, the data should be Fourier analyzed *before* they are recorded to make full use of the 70 db dynamic range of the radar. Currently the data are recorded with a dynamic range of 30-40 db; the collection of FM-CW data at long distances when ground clutter is significant is therefore seriously limited. The solution to this problem is a "smart" pre-processor which can choose the time interval over which the perturbation time series is collected.

We plan to test out a portable CW 35 GHz radar (Pasqualucci et al. 1983; Hobbs et al. 1985) during the spring of 1991 to see if we can improve upon sensitivity when cloud droplets and no precipitation-sized particles are present.

5. ACKNOWLEDGMENTS

NSF grant ATM-8902594, with a subcontract to LANL, funded this research. Our crew on 31 May 1990 consisted of OU undergraduate student Herb Stein, OU graduate students Jim LaDue and Steve Parker, and the first author. Mike Wolf and Roger Bracht at LANL contributed to the design and modification of the radar. Chris Doniec, one of LANL's summer students, was especially helpful in making the FM-CW modification. Steven Cooper, NWS, Amarillo, Texas and Dave Oliver, Channel 7, Amarillo, provided additional documentation of the Spearman tornadoes.

6. REFERENCES

Bluestein, H. B. and W. P. Unruh, 1989: Observations of the wind field in tornadoes, funnel clouds, and wall clouds with a portable Doppler radar. *Bull. Amer. Meteor. Soc.*, *70*, 1514–1525 and cover.

Bluestein, H. B. and W. P. Unruh, 1990: Observations of tornadoes and wall clouds with a portable FM-CW Doppler radar: 1989-1990 results. *Preprints, 16th Conf. on Severe Local Storms*, Kananaskis Park, Alberta, Canada, Amer. Meteor. Soc., 185-188.

Bluestein, H. B. and G. R. Woodall, 1990: Doppler-radar analysis of a low-precipitation severe storm. *Mon. Wea. Rev.*, *118*, 1640-1664.

Brady, H. R. and E. J. Szoke, 1989: A case study of non-mesocyclone tornado development in northeast Colorado: Similarities to waterspout formation. *Mon. Wea. Rev.*, *117*, 843-856.

Hobbs, P. V., N. T. Funk, R. R. Weiss, Sr., J. D. Locatelli, and K. R. Biswas, 1985: Evaluation of a 35 GHz radar for cloud physics research. *J. Atmos. and Ocean. Tech.*, *2*, 35-48.

Pasqualucci, F., B. W. Bartram, R. A. Kropfli, and W. R. Moninger, 1983: A millimeter-wavelength dual-polarization Doppler radar for cloud and precipitation studies. *J. Clim. Appl. Meteor.*, *22*, 758-765.

Roberts, R. D. and J. W. Wilson, 1989: Multiple Doppler radar analysis of the 15 June 1988 Denver tornadoes. *Preprints, 24th Conf. on Radar Meteor.*, Tallahassee, Amer. Meteor. Soc., 142-145.

Strauch, R. G., 1976: Theory and Application of the FM-CW Doppler radar. Ph. D. thesis, Dept. of Electrical Engineering, Univ. of Colo., Boulder, 97 pp.

Unruh, W. P., M. A. Wolf, and H. B. Bluestein, 1989: A portable CW/FM-CW Doppler radar for local investigation of severe storms. *Preprints, 24th Conf. on Radar Meteor.*, Tallahassee, Amer. Meteor. Soc., 634-636.

Wakimoto, R. and J. Wilson, 1989: Non-supercell tornadoes. *Mon. Wea. Rev., 117*, 1113-1140.

Wilson, J. W. and R. D. Roberts, 1990: Vorticity evolution of a non-supercell tornado on 15 June 1988 near Denver. *Preprints,16th Conf. on Severe Local Storms*, Kananaskis Park, Alberta, Canada, Amer. Meteor. Soc., 479-484.

Zrnic, D. S. and R. J. Doviak, 1975. Velocity spectra of vorticies scanned with a pulse-Doppler radar. *J. Appl. Meteor., 14*, 1531-1539.

Zrnic, D. S., R. J. Doviak, and D. W. Burgess, 1977: Probing tornadoes with a pulse Doppler radar. *Quart. J. Roy. Meteor. Soc., 103*, 707-720.

Zrnic, D. S. and M. Istok, 1980: Wind speeds in two tornadic storms and a tornado, deduced from Doppler spectra. *J. Appl. Meteor., 19*, 1405-1415.

Zrnic, D. S., D. W. Burgess, and L. Hennington, 1985: Doppler spectra and estimated windspeed of a violent tornado. *J. Clim. Appl. Meteor., 24*, 1068-1081.

Fig. 1: Photograph of a tornado east of Spearman, Texas at 1909 CDT, looking toward the west from 2 mi west of Highway 70, on FM 759. (photograph by Howard B. Bluestein)

Fig. 2: CW spectrum of the tornado shown in Fig. 2, several min later. Ordinate is the relative spectral density plotted logarithmically. The noise level is indicated by a horizontal line; the linear spectral dropoff (which is exponential with respect to a linear ordinate) is indicated by a sloping solid line.

Fig. 3: As in Fig. 2, but for the left side of the tornado, and fewer spectra have been

averaged.

Fig. 4: As in Fig. 3, but for the right side of the tornado.

Fig. 5: FM-CW spectra of the wall cloud associated with the storm that had approximately10-20 min earlier produced the tornado shown in Fig. 1 plotted as a function of range every 78 m between (a) 1950 m and 2496 m and (b) 2574 and 3120 m. The ordinate is relative spectral density plotted on a logarithmic scale.

Fig. 6: Integrated relative spectral density (logarithmic ordinate) as a function of Doppler velocity for the wall cloud discussed in Fig. 5.

Fig. 7: CW relative spectral density (logarithmic ordinate) as a function of Doppler velocity for the wall cloud discussed in Fig. 5.

Fig. 1

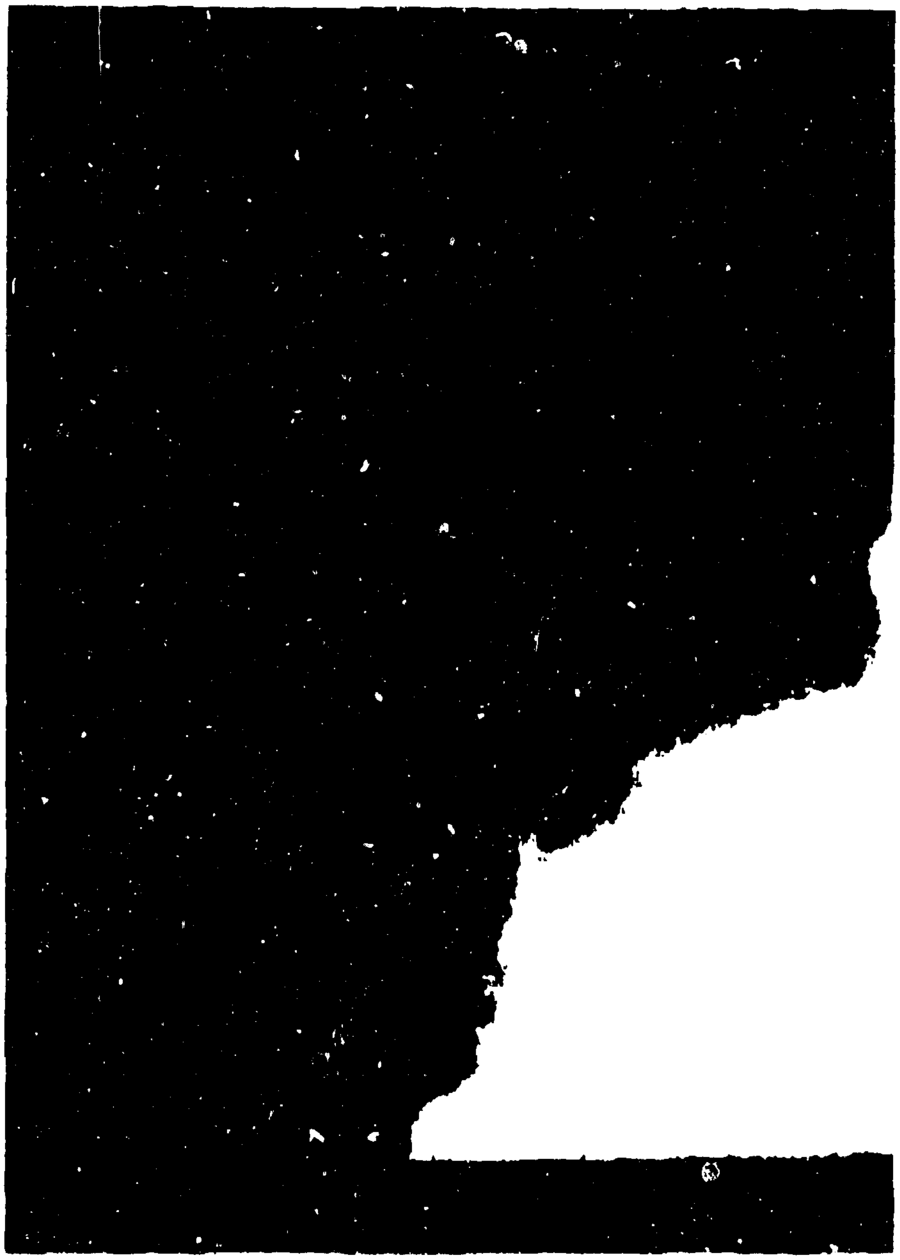

Fig. 2

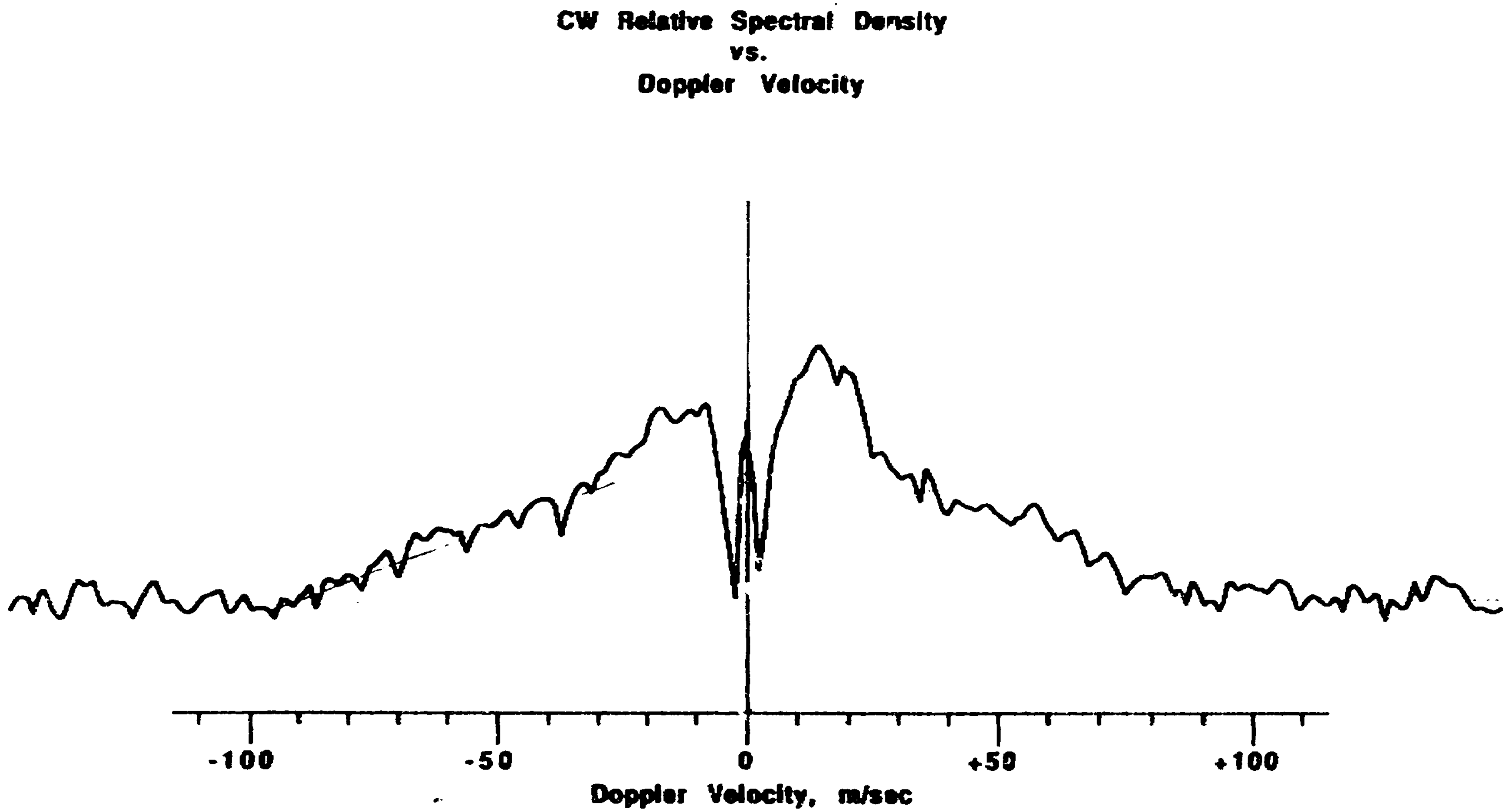

CW Relative Spectral Density
vs.
Doppler Velocity
-100
-50
0
+50
+100
Doppler Velocity, m/sec

Fig 3

CW Relative Spectral Density
vs.
Doppler Velocity

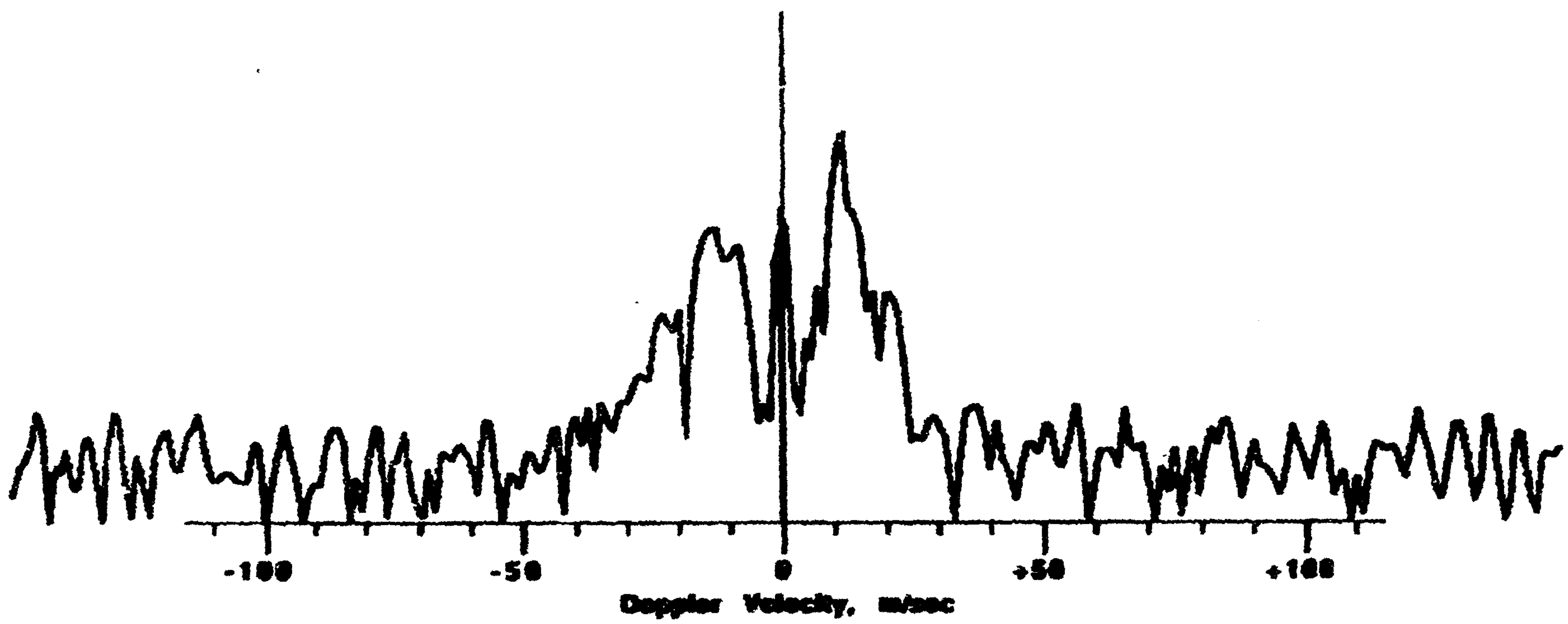

CW Relative Spectral Density
vs.
Doppler Velocity

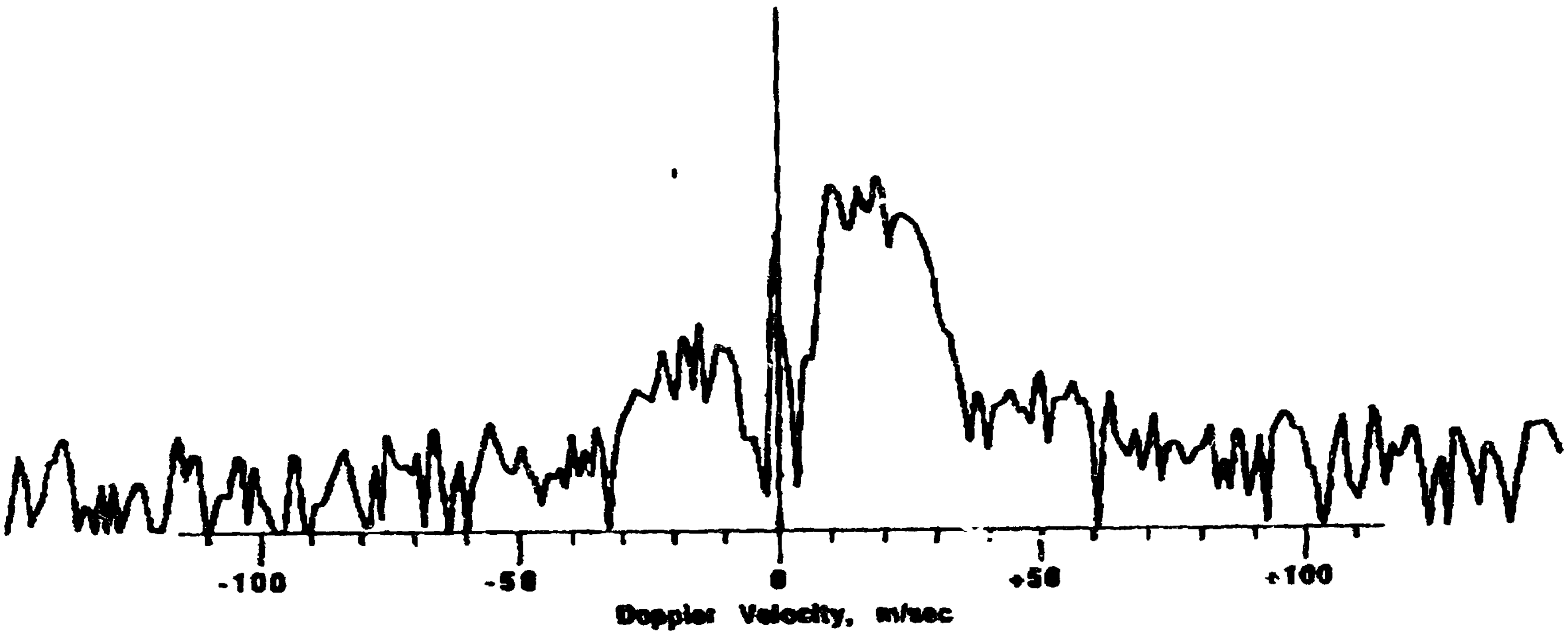

File sp882.3.c.f
S.F. = .5

Eighth 4, 1024 Points

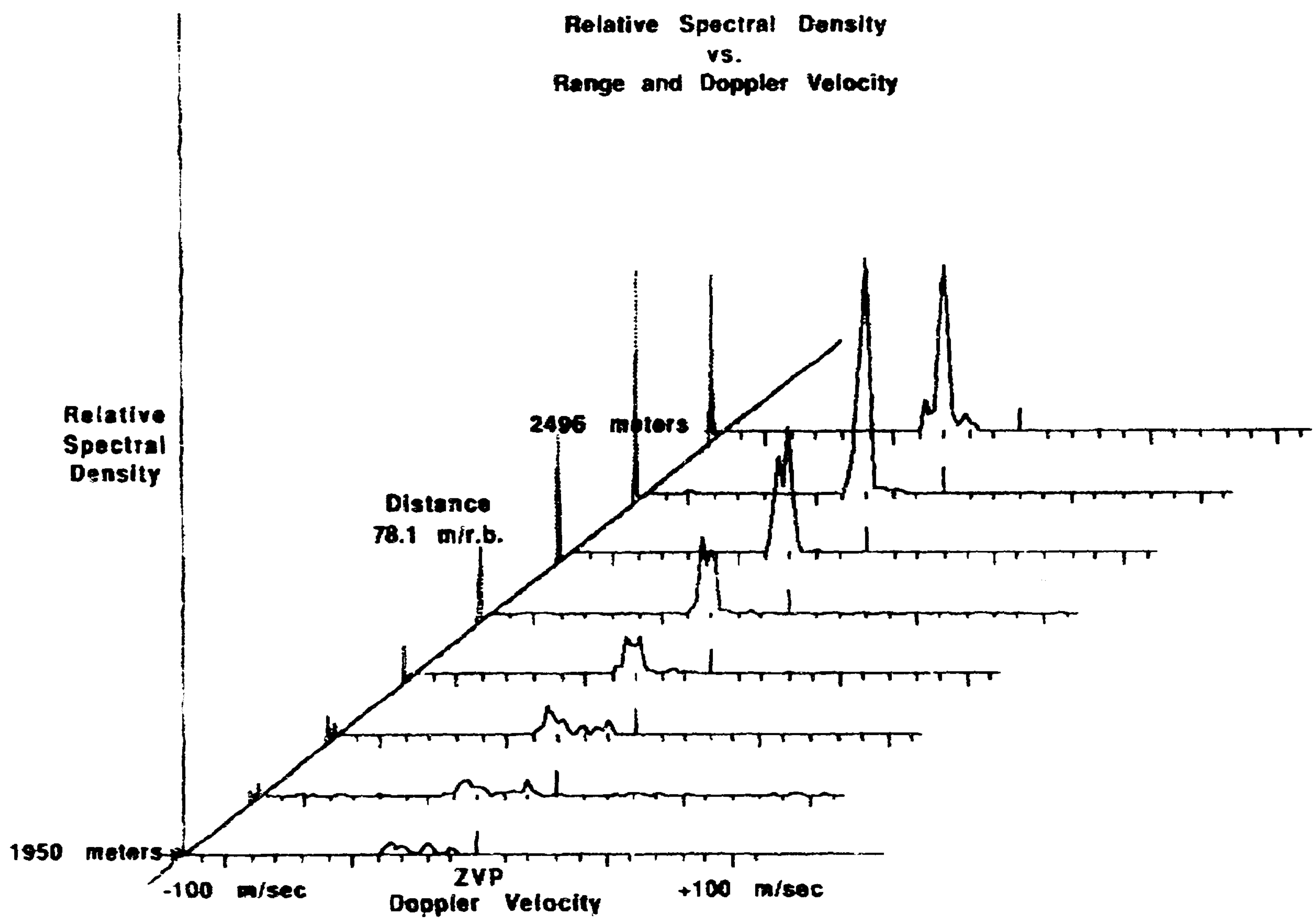

a

File sp882.3.c.f
S.F. = .5

Eighth 5, 1024 Points

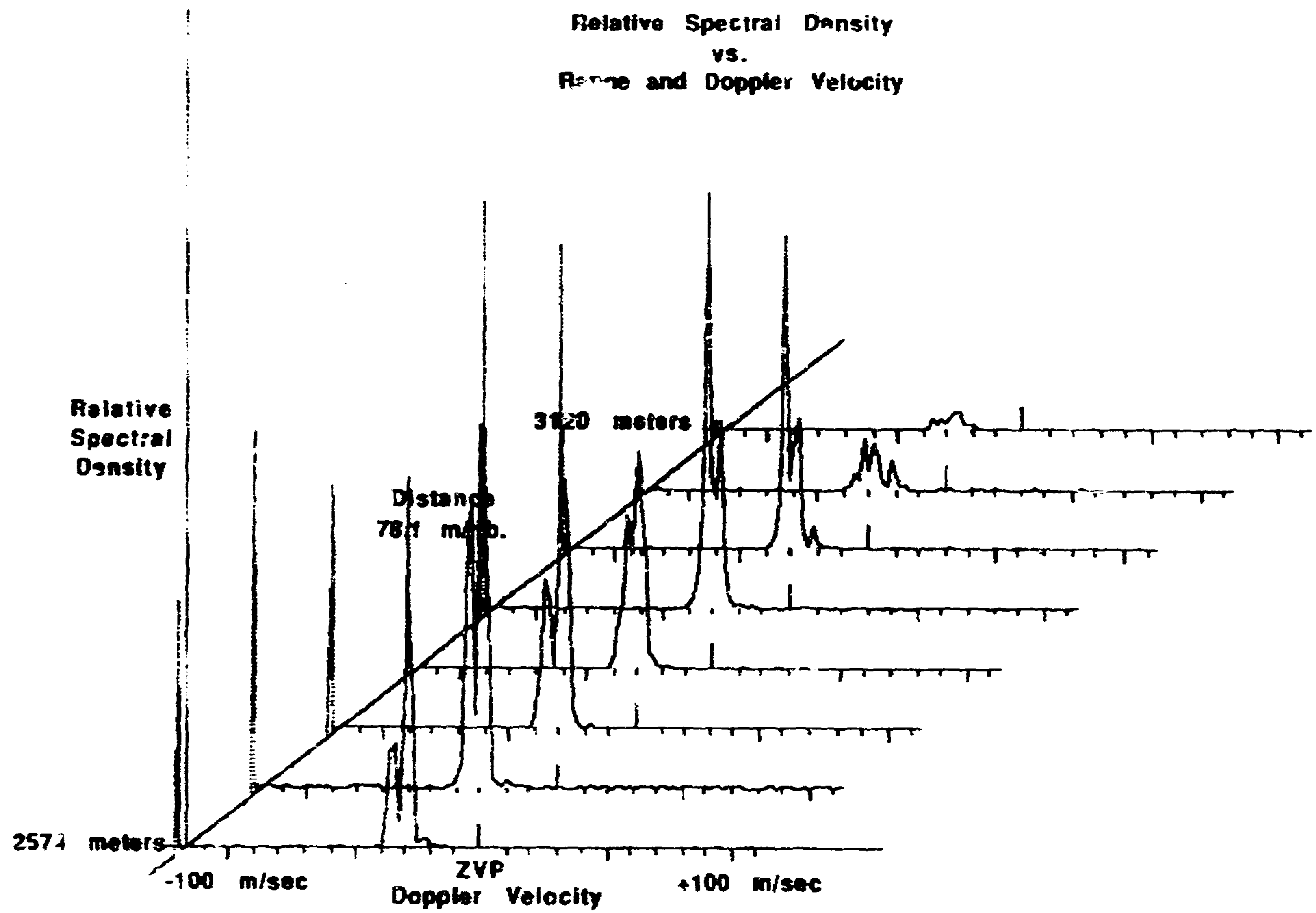

File sp322.3.c.f
S.F. = 1

Integrated Relative Spectral Density
vs.
Doppler Velocity

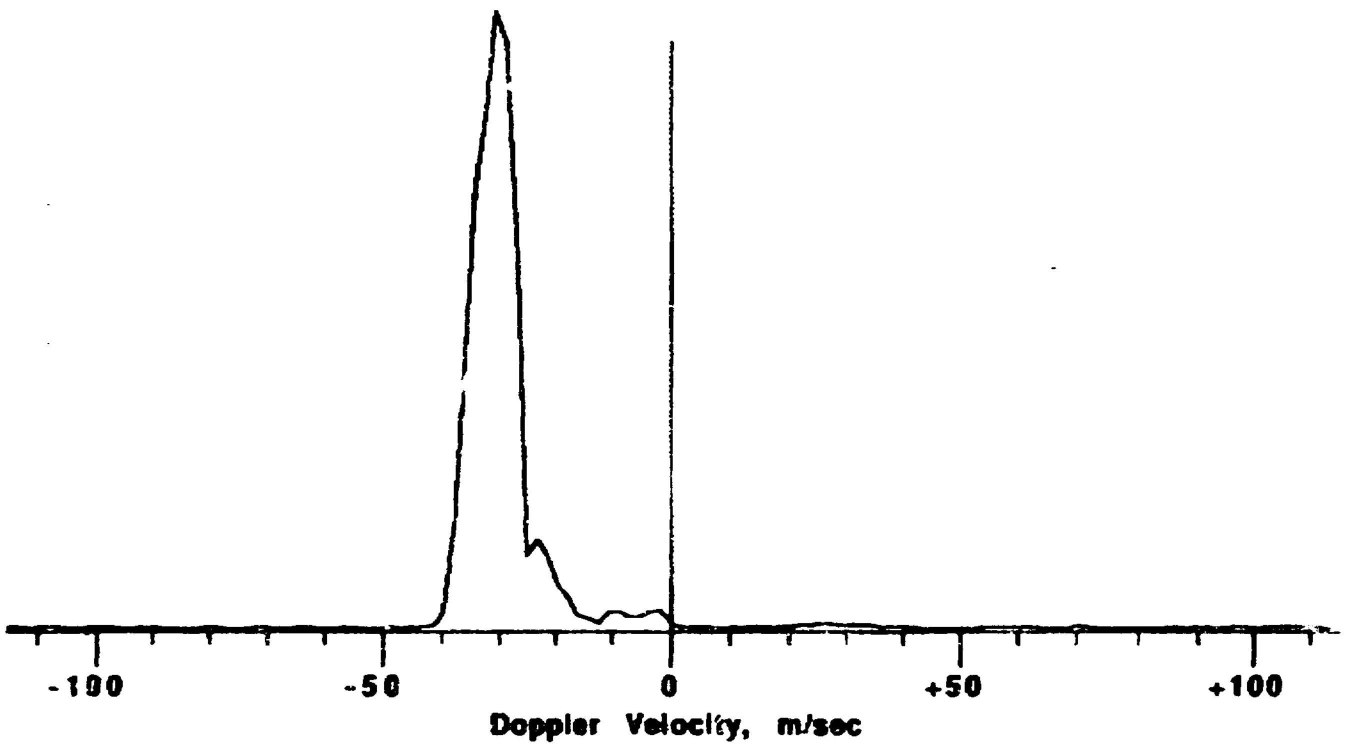

CW Relative Spectral Density
vs.
Doppler Velocity